

Composite-Fermion Theory for Pseudogap, Fermi Arc, Hole Pocket, and Non-Fermi-Liquid of Underdoped Cuprate Superconductors

Youhei Yamaji* and Masatoshi Imada

Department of Applied Physics, University of Tokyo, Hongo, Bunkyo-ku, Tokyo, 113-8656, Japan.

(Dated: October 26, 2018)

We propose that an extension of the exciton concept to doped Mott insulators offers a fruitful insight into challenging issues of the copper oxide superconductors. In our extension, new fermionic excitations called cofermions emerge in conjunction to generalized excitons. The cofermions hybridize with conventional quasiparticles. Then a hybridization gap opens, and is identified as the pseudogap observed in the underdoped cuprates. The resultant Fermi-surface reconstruction naturally explains a number of unusual properties of the underdoped cuprates, such as the Fermi arc and/or pocket formation.

PACS numbers: 71.10.Fd, 71.10.Hf, 71.30.+h, 74.72.-h

Since the discovery of cuprate superconductors, the nature of low-energy electronic excitations evolving in their normal metallic phase has attracted much attention as one of the central issues in condensed matter physics. One reason for the interest lies in its connection to the origin of the high temperature superconductivity itself.

Electronic states in the underdoped cuprates are unconventional. For example, spin and charge excitations are unexpectedly suppressed as “pseudogap phenomena” in the normal state. Recent improvement of experimental tools, such as angle-resolved photoemission spectroscopy (ARPES), has further enabled resolving strong momentum dependence of quasiparticles^{1–3}. In particular, quasiparticles are hardly observed around antinodal points $(\pi, 0)$ and $(0, \pi)$ in the 2D Brillouin zone for the CuO_2 plane. It looks a truncation of a large Fermi surface observed in the overdoped cuprates, and is sometimes called the “Fermi arc”. More fundamentally, the normal state of the cuprates remains a challenge as Mott physics in the proximity to the Mott insulator⁴. Although the doped Mott insulators in two dimensions have been studied for a long time from various theoretical approaches^{5–16}, the nature of the electronic states is not yet fully understood. Recently revealed pseudogap and arc or pocket of the Fermi surface^{1–3} require a conceptually deeper understanding for Mott physics.

In this letter, we elucidate a key role of exciton-like physics on this issue. Excitons are known to be a key concept in physics of semiconductors^{17,18}. The excitonic state also emerges in the Mott insulator, for instance as the charge transfer excitation at the optical gap edge in the cuprates^{19–21}, due to a strong binding of empty (holon) and doubly occupied (doublon) sites in half-filled Mott insulators. In the doped Mott insulators, in spite of screening by doped carriers, the remnant of the binding may still remain as weak binding between a doped holon and the preexisting doublons similarly to excitons. When an electron or hole is added to the doped Mott insulators, it may appear as a normal quasiparticle extended in space. However, an electron (a hole) can alternatively be added locally to a holon (doublon) site with a small cost of the on-site Coulomb repulsion. This generates a bound

composite particle (cofermion) consisting of the preexisting holon (doublon) and the added electron (hole). We call such cofermions *holo-electron* (*doublo-hole*).

A cofermion (a holo-electron or a doublo-hole) dynamically breaks up into (and recombines from) a conventional quasiparticle and a charge boson. This dynamical process is naturally interpreted as a hybridization between the cofermion and the quasiparticle. Here, we show that the resultant hybridization gap offers a natural understanding of a number of key properties of the underdoped cuprates⁴ such as Fermi pocket or arc formation^{1–3}, pseudogap behavior seen in the single particle spectra^{2,22}, specific heat^{23,24}, the asymmetric density of states (DOS)²⁵, and violation of the Wiedemann-Franz law^{26,27}, without any symmetry breaking. We specifically predict that the pseudogap opens as a *s*-wave-like gap in the *unoccupied* part above the Fermi level contrary to the widely assumed *d*-wave structure.

We study the Hubbard hamiltonian on a square lattice,

$$\hat{H} = \sum_{i,j} t_{ij} \hat{c}_{i\sigma}^\dagger \hat{c}_{j\sigma} + U \sum_i \hat{n}_{i\uparrow} \hat{n}_{i\downarrow}, \quad (1)$$

where $\hat{c}_{i\sigma}^\dagger$ ($\hat{c}_{i\sigma}$) is spin- σ creation (annihilation) operator at a site i , while $\hat{n}_{i\sigma} = \hat{c}_{i\sigma}^\dagger \hat{c}_{i\sigma}$. For the hopping t_{ij} , we take only $-t$ for the nearest-neighbor and t' for the next-nearest-neighbor pairs.

We first employ the Kotliar-Ruckenstein slave-boson formalism²⁸, while the local Hilbert space of the Hubbard model is expanded not by the original electron \hat{c}_σ but instead by introducing a fermion \hat{f}_σ , which stands for the σ -spin quasiparticle, following Ref.29 and one slave boson for each Fock state as \hat{e} for the empty state (holon) $|0\rangle$, \hat{p}_σ for the singly occupied state $|\sigma\rangle$ ($\sigma=\uparrow$, or \downarrow), and \hat{d} for the doubly occupied state (doublon) $|\uparrow\downarrow\rangle$. After the mapping, the Coulomb repulsion U is now interpreted as a “chemical potential” for \hat{d}_i^\dagger , while the correlation now appears, as we describe below, in hopping process of $\hat{f}_{i\sigma}^\dagger$ disturbed by slave-boson motion under the local constraints $\hat{e}_i^\dagger \hat{e}_i + \sum_\sigma \hat{p}_{i\sigma}^\dagger \hat{p}_{i\sigma} + \hat{d}_i^\dagger \hat{d}_i = 1$ and $\hat{f}_{i\sigma}^\dagger \hat{f}_{i\sigma} = \hat{p}_{i\sigma}^\dagger \hat{p}_{i\sigma} + \hat{d}_i^\dagger \hat{d}_i$ imposed to keep consistency be-

tween the boson and fermion Hilbert space. In the enlarged Hilbert space, these two constraints are assured respectively by the Lagrange multipliers $\lambda_i^{(1)}$ and $\lambda_{i\sigma}^{(2)}$ in the Lagrangian as

$$\hat{\mathcal{L}} = \sum_{ij} \hat{f}_{i\sigma}^\dagger(\tau) [\hat{D}_i \delta_{ij} + \hat{\zeta}_{ij\sigma}(\tau) t_{ij}] \hat{f}_{j\sigma}(\tau) + \hat{\mathcal{L}}_B^{(0)}, \quad (2)$$

where $\hat{D}_i = \partial_\tau - \mu + \lambda_{i\sigma}^{(2)}$, $\hat{\zeta}_{ij\sigma}(\tau) = \hat{z}_{i\sigma}(\tau) \hat{z}_{j\sigma}^\dagger(\tau)$, and $\hat{z}_{i\sigma} = \hat{g}_{i\sigma}^{(1)} (\hat{p}_{i\sigma}^\dagger \hat{e}_i + \hat{d}_i^\dagger \hat{p}_{i\sigma}) \hat{g}_{i\sigma}^{(2)}$ ($\hat{g}_{i\sigma}^{(1)} = (1 - \hat{p}_{i\sigma}^\dagger \hat{p}_{i\sigma} - \hat{e}_i^\dagger \hat{e}_i)^{-1/2}$ and $\hat{g}_{i\sigma}^{(2)} = (1 - \hat{p}_{i\sigma}^\dagger \hat{p}_{i\sigma} - \hat{d}_i^\dagger \hat{d}_i)^{-1/2}$, following the literature²⁸). A part of the Lagrangian $\hat{\mathcal{L}}_B^{(0)}$ contains $\lambda_i^{(1)}$, $\lambda_{i\sigma}^{(2)}$ and quadratic terms of bosonic fields only²⁸ as, $\hat{\mathcal{L}}_B^{(0)} = \sum_i \{ \tilde{e}_i^\dagger(\tau) [\partial_\tau + \lambda_i^{(1)}] \tilde{e}_i(\tau) + \sum_\sigma \tilde{p}_{i\sigma}^\dagger(\tau) [\partial_\tau + \lambda_{i\sigma}^{(2)} - \lambda_{i\sigma}^{(2)}] \tilde{p}_{i\sigma}(\tau) + \tilde{d}_i^\dagger(\tau) [\partial_\tau + U + \lambda_i^{(1)} - \sum_\sigma \lambda_{i\sigma}^{(2)}] \tilde{d}_i(\tau) \}$. To take into account the Gaussian fluctuations of the bosonic fields beyond the mean-field level³⁰, the Bogoliubov prescription is useful, where the boson operators \hat{b}_i ($b = e, d$ or p_σ) are divided into condensate \bar{b}_0 and fluctuating components \tilde{b}_i as $\hat{b}_i = \bar{b}_0 + \tilde{b}_i$, $\hat{b}_i = \bar{b}_0 + \tilde{b}_i$.

In this letter, we further make a progress by considering low-energy dynamics arising from coupled bosons and fermions. First, we reexamine the strong coupling ($U/t \rightarrow +\infty$) limit^{8,16}, where adding a σ -spin electron is possible only to $|0\rangle$, namely, a holon site, to avoid creating $|\uparrow\downarrow\rangle$ (doublon) with the cost of U . Creation operators for the electron at $|0\rangle$ are given by composite fermion operators $\tilde{e}_i \hat{f}_{i\sigma}^\dagger$.

When t/U becomes nonzero, an added electron may become a coherent quasiparticle. However, we still have rather localized character of holons, and it allows alternatively forming a collective excitation of a hole and the added electron similarly to an exciton. This collective character is clearly distinguished from the conventional quasiparticle. In fact this composite fermion does not have charge in contrast to the quasiparticle. Our crucial step is to include dynamics of this composite fermion expressed by $\tilde{e}_i \hat{f}_{i\sigma}^\dagger$ ($\hat{f}_{i\sigma}^\dagger \tilde{e}_i$).

When we impose the local constraints more strictly for fluctuating bosons beyond the mean-field level, it turns out that, in the hopping process of \hat{f}_σ expressed by $\hat{f}_{i\sigma}^\dagger \hat{\zeta}_{ij\sigma} t_{ij} \hat{f}_{j\sigma}$, the coefficient $\hat{\zeta}_{ij\sigma}^{(1)} = g_{1\sigma}^2 g_{2\sigma}^2 (\tilde{p}_{i\sigma}^\dagger \tilde{e}_i + \tilde{d}_i^\dagger \tilde{p}_{i\sigma}) (\tilde{e}_j^\dagger \tilde{p}_{j\sigma} + \tilde{p}_{j\sigma}^\dagger \tilde{d}_j)$ is dominating (see Appendix. 1 a). Here we employ $g_{1\sigma} = (1 - \bar{p}_{0\sigma}^2 - \bar{e}_0^2)^{-1/2}$ and $g_{1\sigma} = (1 - \bar{p}_{0\sigma}^2 - \bar{d}_0^2)^{-1/2}$ following Ref.28. This vertex stands for the *backflow* consisting of bosons, originating from the quasiparticle motions.

Then we treat coupling of charge bosons and quasiparticles in $\hat{f}_{i\sigma}^\dagger \hat{\zeta}_{ij\sigma}^{(1)} \hat{f}_{j\sigma}$, which represents a part of the electron-electron interactions in the hamiltonian (1), by interpreting the form such as $\hat{f}_{i\sigma}^\dagger \tilde{b}_i \tilde{b}_j^\dagger \hat{f}_{j\sigma}$ as the decoupled product of $\hat{\mathcal{C}}_{i\sigma}^\dagger = (\tilde{e}_i, \tilde{d}_i) \hat{f}_{i\sigma}^\dagger$ and $\hat{\mathcal{C}}_{i\sigma} = \hat{f}_{i\sigma} (\tilde{e}_i^\dagger, \tilde{d}_i^\dagger)^T$. Namely, this boson-quasiparticle interaction is equivalently treated by introducing integrals over the grass-

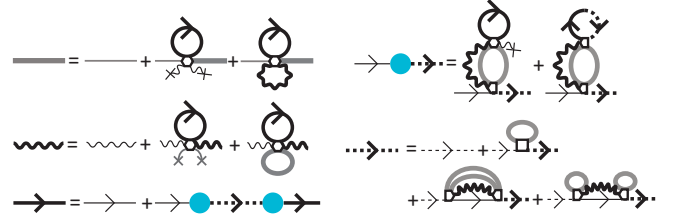


FIG. 1: Diagrams for the Dyson equations. Solid and dashed lines with arrows represent propagators of the quasiparticles and cofermions, respectively. Wavy lines stand for the charge bosons, and solid lines are the spin bosons. Condensations of bosons are represented by lines terminated by crosses. Coupling constant $g_{1\sigma}^2 g_{2\sigma}^2 t_{ij}$ is represented by open polygons. Here, we do not distinguish holons and doublons. Spins and “flavors” of cofermions (ψ, χ) are also not distinguished in the diagram, for simplicity. Filled circles stand for the amplitude of the hybridization between quasiparticles and cofermions.

manian Stratonovich-Hubbard fields $\hat{\mathbf{Y}}_{i\sigma}^\dagger = (\hat{\psi}_{i\sigma}^\dagger, \hat{\chi}_{i\sigma}^\dagger)$ and $\hat{\mathbf{Y}}_{i\sigma} = (\hat{\psi}_{i\sigma}, \hat{\chi}_{i\sigma})^T$ where the interaction is formally transformed to the hybridization of $\hat{\mathbf{Y}}$ and $\hat{\mathcal{C}}$ as $\hat{\mathcal{C}}_{i\sigma}^\dagger \hat{\mathcal{C}}_{j\sigma} \rightarrow \hat{\mathcal{C}}_{i\sigma}^\dagger \hat{\mathbf{Y}}_{j\sigma} + \hat{\mathbf{Y}}_{i\sigma}^\dagger \hat{\mathcal{C}}_{j\sigma} - \hat{\mathbf{Y}}_{i\sigma}^\dagger \hat{\mathbf{Y}}_{j\sigma}$ (see Appendix. 1 b).

The newly introduced Grassmann fields $\hat{\psi}_{i\sigma}^\dagger$ and $\hat{\chi}_{i\sigma}$ are physically interpreted as cofermions, the holo-electron and doublo-hole, respectively. Then, $\hat{\mathcal{C}}_{i\sigma}^\dagger \hat{\mathbf{Y}}_{j\sigma} + \hat{\mathbf{Y}}_{i\sigma}^\dagger \hat{\mathcal{C}}_{j\sigma}$ is naturally interpreted as breakup and recombination processes of the cofermions. After integrating fluctuating bosons out, as is mentioned below, it results in the hybridization between cofermions $\hat{\psi}_\sigma, \hat{\chi}_\sigma$ and quasiparticles \hat{f}_σ .

We treat Gaussian fluctuations of bosons, and the dynamical coupling between quasiparticles and cofermions by using a set of the Dyson equations up to the second order of t_{ij} , as is depicted in Fig.1: Thick lines (thick wavy lines) stand for the dressed Green’s functions of the charge bosons $\mathcal{A}^{ab}(r, \tau) = -\langle T \beta_i^a(\tau) \beta_j^{b\dagger}(0) \rangle$ (spin bosons $\mathcal{C}^{ab}(r, \tau) = -\langle T \phi_i^a(\tau) \phi_j^{b\dagger}(0) \rangle$), where $a, b = 1, 2$, $r = i - j$, $(\beta_i^1, \beta_i^2) = (\tilde{e}_i, \tilde{d}_i)$, and $(\phi_i^1, \phi_i^2) = (\tilde{p}_{i\sigma}, \tilde{p}_{i\sigma}^\dagger)$. Here we neglect the coupling between charge and spin bosons such as $\langle \tilde{p}_{i\sigma}^\dagger \tilde{e}_i \rangle$, which vanishes in Mott insulators and gives higher order terms scaled by the doping rate x for $|x| \ll 1$. Thick lines with arrows represent the dressed quasiparticles $\mathcal{G}_\sigma^{(f)}(r, \tau)$. Thin lines (thin wavy lines) represent bare propagators of the charge bosons $\mathcal{A}_0^{ab}(r, \tau)$ (spin bosons $\mathcal{C}_0^{ab}(r, \tau)$), determined by $\hat{\mathcal{L}}_B^{(0)}$. Thin lines with arrows are bare propagators of the quasiparticles $\mathcal{G}_0^{(f)}(r, \tau)$ determined by $\hat{\mathcal{L}}_0 = \sum_{ij} \hat{f}_{i\sigma}^\dagger(\tau) [\hat{D}_i \delta_{ij} + \zeta_{0\sigma} t_{ij}] \hat{f}_{j\sigma}(\tau)$, where $\zeta_{0\sigma} = g_{1\sigma}^2 g_{2\sigma}^2 (\bar{p}_{0\sigma} \bar{e}_0 + \bar{d}_0 \bar{p}_{0\sigma})^2$. The Lagrangian $\hat{\mathcal{L}}_0$ is obtained by decoupling the fluctuating bosons from the Lagrangian $\hat{\mathcal{L}} - \hat{\mathcal{L}}_B^{(0)}$ (see Eq.(2)). Thick and thin dashed lines with arrows are the cofermion propagators \mathcal{F}^{cd} ($c, d = \psi, \chi$) and $\mathcal{F}_0^{cd} = \delta_{cd}/\epsilon$ ($\epsilon \rightarrow 0$), respectively. This

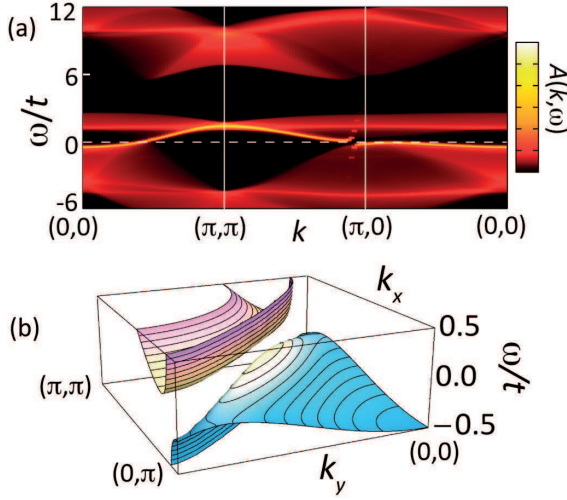


FIG. 2: (color online). Calculated spectral functions for $t'/t=0.25$, $U/t=12$ and $x=0.05$. (a) Spectral function $A(k, \omega)$ along lines running from $(0, 0)$, (π, π) and $(\pi, 0)$ to $(0, 0)$. The dashed line is the Fermi level. We use a finite broadening factor $\delta=0.05t$. (b) Band dispersion of quasiparticle for $x=0.05$.

peculiar divergence of \mathcal{F}_0^{cd} is because the Lagrangian does not include cofermions if we neglect the interactions between bosons and fermions. By solving the Dyson equations, we obtain the propagators for the quasiparticles and cofermions. Here the bosonic degrees of freedom are taken into account in a self-consistent fashion, through the cofermion self-energy and the amplitude of hybridization between the quasiparticles and cofermions.

Now we show how our self-consistent solution of coupled quasiparticles, bosons and cofermions predicts normal state properties. We show the result at $U=12t$ and $t'=0.25t$ to get insight into the cuprate superconductors by restricting to paramagnetic solutions at temperature $T=0$. First, we give the spectral functions calculated from the electron Green's function $G_\sigma(k, \omega)$ (see Appendix. 1 c); $A(k, \omega) = -\text{Im}[G_\sigma(k, \omega)]/\pi$. In Fig.2a, we show $A(k, \omega)$ for the hole concentration $x = 0.05$. Two main features are found; the coherent band arising from the quasiparticle around the Fermi level and the remnant of the upper (lower) Hubbard band at $\omega > 6t$ ($\omega < -2t$) generated by dynamics of \tilde{e} and $\tilde{d}^{30,31}$.

Here, we focus on reconstructions of the Fermi surface in the coherent band. The quasiparticle Green's function is given as

$$G_\sigma^{(f)}(k, \omega) \simeq [\omega - \zeta_{0\sigma}\epsilon_k + \mu - \Sigma_f(k, \omega)]^{-1}, \quad (3)$$

where $\Sigma_f = \Delta(k)^2/(\gamma_k\omega - \alpha_k)$ is the quasiparticle self-energy arising from the quasiparticle-cofermion hybridization $\Delta(k)$. Here the cofermion propagator $(\gamma_k\omega - \alpha_k)^{-1}$ is obtained from the expansion around the cofermion pole (see Appendix. 1 c). The quasiparticles Green's function has a hybridization gap due to the hy-

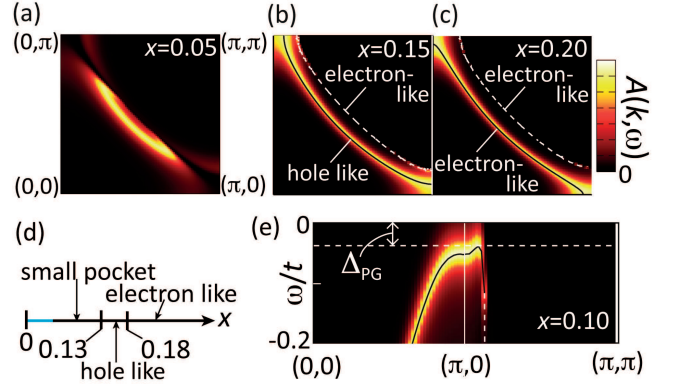


FIG. 3: (color online). Reconstructed Fermi surfaces and spectral functions $A_f(k, \omega)$ for $t'/t=0.25$ and $U/t=12$. (a)-(c) $A_f(k, \omega) (\equiv -\text{Im}[G_\sigma^{(f)}(k, \omega)]/\pi)$ at $\omega = i\delta$. Here we take the broadening factor $\delta = 0.05t$. Solid and dashed lines illustrate the poles of quasiparticles. (d) Doping dependence of Fermi-surface topology in our theory. (e) $A_f(k, \omega)$ along the symmetry line running from $(0, 0)$ through $(\pi, 0)$ to (π, π) for $x = 0.10$. Thin solid and dashed white lines illustrate poles of quasiparticles. We define Δ_{PG} as the gap between μ ($\omega = 0$) and the maximum of the quasiparticle dispersion below μ along this symmetry line.

bridization with the cofermions and $G_\sigma^{(f)}$ shows the divergence of the quasiparticle self-energy given by Σ_f at the zero surface^{11,13-15} defined by $\gamma_k\omega - \alpha_k = 0$. In our theory, the zero surface splits the band dispersion and generates a distinct s -wave-like gap (as is seen in Fig.2b and supported by recent numerical observation^{14,15}). For small hole doping such as $x=0.05$, our theory predicts that the reconstructed Fermi surface becomes a small pocket as we see in Fig.3a-3c.

Actually, the topological transitions occur at $x \simeq 0.13$ and $x \simeq 0.18$ (see Fig.3d). Below $x \simeq 0.13$, the Fermi surface consists of small hole pockets. It is difficult to distinguish the pockets from the arc structure as we see in Fig.3a. This is because the zero surface near the outer part partially destroys the quasiparticles. For $0.13 \lesssim x$, large Fermi surfaces appear, instead of Fermi pockets. For $0.13 \lesssim x \lesssim 0.18$, a hole-like surface centered at (π, π) , and an electron-like one centered at (π, π) coexist (see Fig.3b). However, the electron-like surface is hardly seen again because of the nearby zero surface. Our result shows a nontrivial topological transition at $x \simeq 0.13$ as a consequence of the hybridization with cofermions.

A gap Δ_{PG} measured from the Fermi level μ emerges near the antinode, corresponding to the pseudogap in the ARPES as we identify in Fig.3e. The pseudogap Δ_{PG} is determined by the hybridization gap $\Delta(k)$, basically scaled by a fraction of t , consistently with numerical studies¹². The doping dependence of Δ_{PG} is given in Fig.4a, in agreement with the ARPES for LSCO^{2,22}.

For $x \lesssim 0.13$, the density of states (DOS) of the electrons $\hat{c}_{k\sigma}$ at the Fermi level, $\rho_F \simeq -\zeta_0 \int d^2k A_f(k, 0)/4\pi^3$,

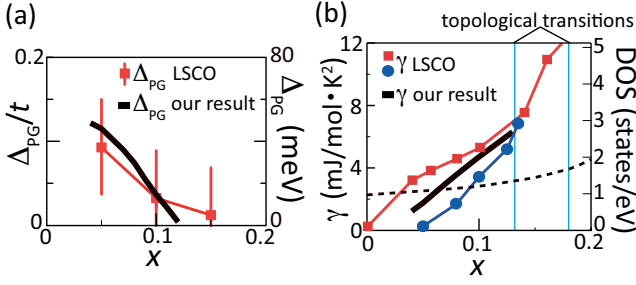


FIG. 4: (color online). (a) Pseudogap Δ_{PG} as a function of hole doping rate x . Thick solid line is Δ_{PG} calculated by our theory. Closed (red) squares show Δ_{PG} estimated from the ARPES²² for $\text{La}_{2-x}\text{Sr}_x\text{CuO}_4$ (LSCO). (b) DOS of electrons vs. x in the present theory (bold solid curve). The thin dashed curve stands for the DOS of the non-interacting case. Closed (blue) circles are obtained by a linear extrapolation of low-temperature normal-state γ of LSCO in Ref.23 to $T \rightarrow 0$, representing the presumable lower limit. Closed (red) squares stand for the estimate for LSCO obtained in Ref.24 by the Zn doping, which may be an upper limit. All of the present results are obtained at $t=0.4\text{eV}$, $t'/t=0.25$ and $U/t=12$.

is clearly suppressed, as is illustrated in Fig.4b. We compare ρ_F with the specific heat coefficient γ measured for LSCO^{23,24} by using the conventional relation $\gamma = \pi^2 \rho_F / 3$ at $T=0$. Our γ is consistent with experiments. The ω -dependence of the DOS shows significant asymmetry around $\omega=0$ in contrast to the DOS for the non-interacting case (see Appendix. 2). This asymmetry of the DOS naturally explains the asymmetric tunneling spectra observed in the hole-underdoped cuprates²⁵ (see Refs.32 and 33 for different interpretations).

The present result slightly depends on the choice of the parameters. For instance, Δ_{PG} decreases from the present result by an amount $\sim 0.05t$ at $t'/t=0.25$ and $U/t=15$ or $t'/t=0.15$ and $U/t=12$, while the qualitative features are robust.

Here we note the difference of the cofermion from the spinon⁹: Although the cofermion carries a spin but no charge as in the spinon, cofermions coexist with quasiparticles in different part of energy-momentum space as the electron differentiation in contrast to the spinons.

The present cofermion contributes to the entropy and the thermal conductivity κ in addition to the quasiparticle. On the other hand, the electric conductivity σ is contributed only from the quasiparticle. Therefore we expect a serious breakdown of the Wiedeman-Franz law^{26,27} that predicts a universal constant $L_0 = \pi^2 k_B^2 / 3e^2$ for the ratio $L \equiv \kappa / T\sigma$. Our theory predicts $L > L_0$.

We propose to test our specific prediction of the s -wave-like gap structure in unoccupied spectra, for example, by improving the low-energy electron spectroscopies, such as the inverse photoemission, the low-energy electron diffraction spectroscopy, resonant inelastic X-ray spectroscopy, or time resolved photoemission spectroscopy. The mid-infrared peak and long tail of the

optical conductivity¹⁹ indeed supports our prediction.

Our finding is that hidden cofermionic particles called *holo-electrons* and *doublo-holes* play a key role: The cofermions hybridize with the quasiparticles and cause a hybridization gap identified as the pseudogap. A number of resultant properties consistent with the unusual normal states of the cuprates support relevance of our cofermion theory to physics of the cuprates.

The authors thank Yukitoshi Motome and Shiro Sakai for useful discussions. Y.Y. is supported by the Japan Society for the Promotion of Science.

Appendix

In this Appendix, we show theoretical details on introducing the cofermions, construction of quasiparticle Green's functions, and supplementary results on the quasiparticle density of states.

1. Details of theory

As our theoretical starting point, we employ the Kotliar-Ruckenstein slave-boson formalism²⁸ for the Hubbard model, where the local Hilbert space of the Hubbard model is expanded by introducing one slave boson for each Fock state as \hat{e} for the empty state (holon) $|0\rangle$, \hat{p}_σ for the singly occupied state $|\sigma\rangle$ ($\sigma=\uparrow$, or \downarrow), and \hat{d} for the doubly occupied state (doublon) $|\uparrow\downarrow\rangle$. In addition to these bosons \hat{b} ($b = e, p_\sigma$ or d), fermion operator \hat{f}_σ is introduced to stand for the σ -spin QP. The mapping between the original electrons and \hat{f} combined with \hat{b} is given by $\hat{c}_{i\sigma}^\dagger \doteq \hat{z}_{i\sigma} \hat{f}_{i\sigma}^\dagger$, where $\hat{z}_{i\sigma}$ is defined^{28,31} as

$$\hat{z}_{i\sigma} = \hat{g}_{i\sigma}^{(1)} (\hat{p}_{i\sigma}^\dagger \hat{e}_i + \hat{d}_i^\dagger \hat{p}_{i\bar{\sigma}}) \hat{g}_{i\sigma}^{(2)} \quad (\text{A.1})$$

with

$$\hat{g}_{i\sigma}^{(1)} = (1 - \hat{p}_{i\bar{\sigma}}^\dagger \hat{p}_{i\bar{\sigma}} - \hat{e}_i^\dagger \hat{e}_i)^{-1/2}, \quad (\text{A.2})$$

and

$$\hat{g}_{i\sigma}^{(2)} = (1 - \hat{p}_{i\sigma}^\dagger \hat{p}_{i\sigma} - \hat{d}_i^\dagger \hat{d}_i)^{-1/2}, \quad (\text{A.3})$$

following the literature²⁸.

We need to impose local constraints to eliminate unphysical states. First, only one boson should occupy each local state as

$$\hat{e}_i^\dagger \hat{e}_i + \sum_\sigma \hat{p}_{i\sigma}^\dagger \hat{p}_{i\sigma} + \hat{d}_i^\dagger \hat{d}_i = 1. \quad (\text{A.4})$$

Second, the number operator of \hat{f}_σ is necessarily given as

$$\hat{f}_{i\sigma}^\dagger \hat{f}_{i\sigma} = \hat{p}_{i\sigma}^\dagger \hat{p}_{i\sigma} + \hat{d}_i^\dagger \hat{d}_i. \quad (\text{A.5})$$

These constraints are represented by integrals over Lagrange multipliers $\lambda_i^{(1)}$, and $\lambda_i^{(2)}$, in the path integral of the Lagrangian discussed below.

In the expanded Hilbert space, the Lagrangian of the Hubbard Hamiltonian is mapped to

$$\hat{\mathcal{L}} = \sum_{ij} \hat{f}_{i\sigma}^\dagger(\tau) [\hat{D}_i \delta_{ij} + \hat{\zeta}_{ij\sigma}(\tau) t_{ij}] \hat{f}_{j\sigma}(\tau) + \hat{\mathcal{L}}_B^{(0)}, \quad (\text{A.6})$$

where $\hat{D}_i = \partial_\tau - \mu + \lambda_{i\sigma}^{(2)}$ and $\hat{\zeta}_{ij\sigma}(\tau) = \hat{z}_{i\sigma}(\tau) \hat{z}_{j\sigma}^\dagger(\tau)$. $\hat{\mathcal{L}}_B^{(0)}$ contains $\lambda_i^{(1)}$, $\lambda_{i\sigma}^{(2)}$ and quadratic terms of bosonic fields only²⁸ as,

$$\begin{aligned} \hat{\mathcal{L}}_B^{(0)} = & \sum_i \{ \tilde{e}_i^\dagger(\tau) [\partial_\tau + \lambda_i^{(1)}] \tilde{e}_i(\tau) \\ & + \sum_\sigma \tilde{p}_{i\sigma}^\dagger(\tau) [\partial_\tau + \lambda_i^{(1)} - \lambda_{i\sigma}^{(2)}] \tilde{p}_{i\sigma}(\tau) \\ & + \tilde{d}_i^\dagger(\tau) [\partial_\tau + U + \lambda_i^{(1)} - \sum_\sigma \lambda_{i\sigma}^{(2)}] \tilde{d}_i(\tau) \}. \end{aligned} \quad (\text{A.7})$$

The on-site Coulomb U is now interpreted as a “chemical potential” for \tilde{d}_i^\dagger , while the correlation now appears in hopping process of $\tilde{f}_{i\sigma}^\dagger$ disturbed by slave boson motion.

a. Bosonic fluctuations

To take into account the Gaussian fluctuations of the bosonic fields beyond the mean-field level³⁰, the Bogoliubov prescription is useful, where the boson operators are divided into condensate components \bar{b}_0 and fluctuating components \tilde{b}_i as $\hat{b}_i^\dagger = \bar{b}_0 + \tilde{b}_i^\dagger$, $\hat{b}_i = \bar{b}_0 + \tilde{b}_i$ with $b = e, d$ or p_σ .

When we impose the local constraints more strictly for fluctuating bosons beyond the mean-field level, it turns out that the term

$$\hat{\zeta}_{ij\sigma}^{(1)} = g_{1\sigma}^2 g_{2\sigma}^2 (\tilde{p}_{i\sigma}^\dagger \tilde{e}_i + \tilde{d}_i^\dagger \tilde{p}_{i\sigma}) (\tilde{e}_j^\dagger \tilde{p}_{j\sigma} + \tilde{p}_{j\sigma}^\dagger \tilde{d}_j) \quad (\text{A.8})$$

represented by the diagram in Fig.5a is dominating among all the possible diagrams for $\hat{\zeta}_{ij\sigma}$ in Eq.(A.6). Here we employ $g_{1\sigma}^2 = (1 - \bar{p}_{0\sigma}^2 - \bar{e}_0^2)^{-1}$ and $g_{2\sigma}^2 = (1 - \bar{p}_{0\sigma}^2 - \bar{d}_0^2)^{-1}$ by following Ref.28.

To elucidate why we retain $\hat{\zeta}_{ij\sigma}^{(1)}$, we classify the diagrams illustrated in Fig.5 into four types, categorized by time dependence (or frequency dependence) of quasiparticles and the local conservation of the boson densities:

(T-1) Diagrams containing external propagators of quasiparticles, in addition to bosonic propagators violating the local conservation of boson densities (Figures 5b, 5c, 5d, and 5h). Here the violation means that before and after the interactions (represented by hexagons), the number of bosons expressed by external boson propagators is not the same.

(T-2) Diagrams that contain time dependence of quasiparticles, but that do not violate the local conservation (Figures 5a and 5e).

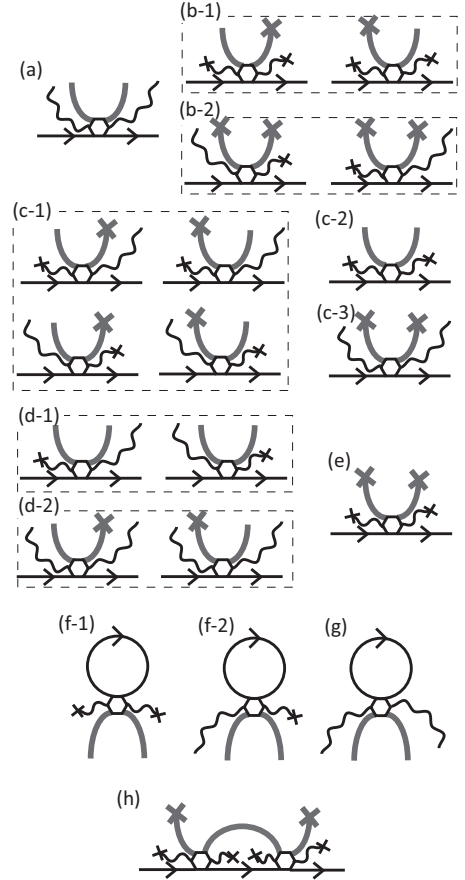


FIG. 5: (a)-(e) Diagrams representing terms in $\hat{f}_{i\sigma}^\dagger \hat{\zeta}_{ij\sigma} \hat{f}_{j\sigma}$. (f)-(h), Examples of the diagrams for perturbation generated from the same term as (a)-(e). Solid lines with arrows represent propagators of the quasiparticles. Wavy lines stand for the charge bosons, and solid lines are the spin bosons. Condensations of bosons are represented by lines terminated at crosses. Coupling constant $g_{1\sigma}^2 g_{2\sigma}^2 t_{ij}$ is represented by open polygons. Here, we do not distinguish holons and doublons. Spins are also not distinguished in the diagram, for simplicity.

(T-3) Diagrams that do not contain time dependence of quasiparticles but do violate the local conservation (Fig.5f).

(T-4) Diagrams that neither include time dependence of quasiparticles nor violate the local conservation (Fig.5g).

Here we present our guiding principle to take account of boson fluctuations: We exclude **(T-1)** because it violates the local conservation when the quasiparticles dynamically fluctuate. On the other hand we retain diagrams belonging to the categories **(T-2)**, **(T-3)**, and **(T-4)**. The reason to retain these diagram is as follows. The diagrams in the category **(T-2)** do not violate the local conservation, when bosons fluctuate. Therefore, we take the diagrams in this category into account. On the

other hand, the diagrams in the category **(T-3)** do violate the local conservation. However, in these diagrams, quasiparticles enter as time averaged Green's functions. Therefore, quasiparticles feel the time averaged bosonic motions. The real violation of the local conservation occurs only when a dynamical quasiparticle process is induced by fluctuating boson hoppings. On the contrary, the real violation does not occur when the quasiparticles emerge as the time averaged quantities as in the case of **(T-3)**. This is the reason to retain the diagrams in the category **(T-3)**. Since **(T-4)** does not violate local conservation, we retain it.

For the slave-particle formalism of correlated fermion systems, it is well-known that fluctuations of gauge fields play an important role on reinforcing the local constraint imposed on slave particles⁹. It was pointed out by Jolicœur and Le Guillou that the Kotliar-Ruckenstein formalism has the $U(1) \times U(1) \times U(1)$ gauge symmetry³⁴. It comes from the phase symmetry of the slave bosonic particles, namely, \hat{e}_i , $\hat{p}_{i\sigma}$, and \hat{d}_i .

In our theory, we will treat fluctuations of such phases together with fluctuations of the amplitude of the condensation fraction of these slave particles, by using the Bogoliubov prescription. Therefore, the phase fluctuations are taken into account, although the $U(1) \times U(1) \times U(1)$ gauge structure is not strictly conserved.

b. Stratonovich-Hubbard transformation

We introduce Grassmannian valuables (or fermionic fields) $\hat{\mathbf{Y}}_{i\sigma} = (\hat{\psi}_{i\sigma}, \hat{\chi}_{i\sigma})^T$ that stands for the cofermions as are discussed in the main article, by using a following identity

$$\int \prod_{i\sigma} d\hat{\mathbf{Y}}_{i\sigma}^\dagger d\hat{\mathbf{Y}}_{i\sigma} e^{\mathcal{A}} = \det[\tilde{\mathbf{T}}_\uparrow \tilde{\mathbf{T}}_\downarrow], \quad (\text{A.9})$$

where matrices $\tilde{\mathbf{T}}_\sigma$ are defined as

$$(\tilde{\mathbf{T}}_\sigma)_{ij} = g_{1\sigma}^2 g_{2\sigma}^2 t_{ij} \begin{bmatrix} \hat{p}_{i\sigma}^\dagger \tilde{p}_{j\sigma} & \hat{p}_{i\sigma}^\dagger \tilde{p}_{j\bar{\sigma}}^\dagger \\ \tilde{p}_{i\bar{\sigma}} \tilde{p}_{j\sigma} & \tilde{p}_{i\bar{\sigma}} \tilde{p}_{j\bar{\sigma}}^\dagger \end{bmatrix}, \quad (\text{A.10})$$

and

$$\begin{aligned} \mathcal{A} = & \int_0^\beta d\tau \sum_{i,j\sigma} \left[\left(\hat{\mathbf{Y}}_{i\sigma}^\dagger(\tau) - \hat{\mathbf{C}}_{i\sigma}^\dagger(\tau) \right) \right. \\ & \times \left. (\tilde{\mathbf{T}}_\sigma)_{ij} \left(\hat{\mathbf{Y}}_{j\sigma}(\tau) - \hat{\mathbf{C}}_{j\sigma}(\tau) \right) \right]. \end{aligned} \quad (\text{A.11})$$

Here we use vector notations as are defined in the main article as

$$\hat{\mathbf{C}}_{i\sigma}^\dagger = (\tilde{e}_i, \tilde{d}_i^\dagger) \hat{f}_{i\sigma}, \quad \hat{\mathbf{C}}_{i\sigma} = \hat{f}_{i\sigma} (\tilde{e}_i^\dagger, \tilde{d}_i)^T. \quad (\text{A.12})$$

The identity Eq.(A.9) gives the transformation for a coupling term of the quasiparticles and fluctuating



FIG. 6: Diagrams for the transformed Lagrangians. Solid and dashed lines with arrows represent propagators of the quasiparticles and cofermions, respectively. Wavy lines stand for the charge bosons, and solid lines are the spin bosons. (a) The diagram represents the Lagrangian \mathcal{L}'_{a1} (Eq.(A.16)). (b) The diagrams stand for terms in the Lagrangian \mathcal{L}'_{a2} (Eq.(A.17)).

bosons depicted in Fig.5a,

$$\mathcal{L}_a = \sum_{ij\sigma} \hat{\mathbf{C}}_{i\sigma}^\dagger(\tau) (\tilde{\mathbf{T}}_\sigma)_{ij} \hat{\mathbf{C}}_{j\sigma}(\tau), \quad (\text{A.13})$$

as

$$\exp \left[- \int_0^\beta d\tau \mathcal{L}_a \right] = \frac{\int \prod_{i\sigma} d\hat{\mathbf{Y}}_{i\sigma}^\dagger d\hat{\mathbf{Y}}_{i\sigma} e^{- \int_0^\beta d\tau \mathcal{L}'_a}}{\det[\tilde{\mathbf{T}}_\uparrow \tilde{\mathbf{T}}_\downarrow]} \quad (\text{A.14})$$

where

$$\mathcal{L}'_a = \mathcal{L}'_{a1} + \mathcal{L}'_{a2}, \quad (\text{A.15})$$

$$\mathcal{L}'_{a1} = \sum_{ij\sigma} \hat{\mathbf{Y}}_{i\sigma}^\dagger(\tau) (\tilde{\mathbf{T}}_\sigma)_{ij} \hat{\mathbf{Y}}_{j\sigma}(\tau), \quad (\text{A.16})$$

$$\begin{aligned} \mathcal{L}'_{a2} = & - \sum_{ij\sigma} \left\{ \hat{\mathbf{C}}_{i\sigma}^\dagger(\tau) (\tilde{\mathbf{T}}_\sigma)_{ij} \hat{\mathbf{Y}}_{j\sigma}(\tau) \right. \\ & \left. + \hat{\mathbf{Y}}_{i\sigma}^\dagger(\tau) \tilde{\mathbf{T}}_{ij} \hat{\mathbf{C}}_{j\sigma}(\tau) \right\}. \end{aligned} \quad (\text{A.17})$$

These transformed Lagrangian \mathcal{L}'_{a1} (Fig.6a) and \mathcal{L}'_{a2} (Fig.6b) lead to the cofermions' self-energy and the hybridization between the quasiparticles and cofermions, respectively after integrating out the fluctuating bosonic degrees of freedom. It will be discussed below, by using a set of the Dyson equations.

c. Prescription for self-consistent procedure and Green's functions

Here we construct approximated Green's functions for the Gaussian fluctuations of the bosons, quasiparticles, and cofermions by using a set of the Dyson equations as is depicted in Fig.7: Thick lines and thick wavy lines stand for the Green's functions of the charge bosons $\mathcal{A}^{ab}(r, \tau) = - \langle T \beta_i^a(\tau) \beta_j^{b\dagger}(0) \rangle$, and the spin bosons $\mathcal{C}^{ab}(r, \tau) = - \langle T \phi_i^a(\tau) \phi_j^{b\dagger}(0) \rangle$, respectively, where $a, b = 1, 2$, $r = i - j$, $(\beta_i^1, \beta_i^2) = (\tilde{e}_i, \tilde{d}_i)$, and $(\phi_i^1, \phi_i^2) =$

$(\tilde{p}_{i\sigma}, \tilde{p}_{i\sigma}^\dagger)$. Thick lines with arrows represent the quasiparticles $\mathcal{G}_\sigma^{(f)}(r, \tau)$. On the other hand, Thin lines and thin wavy lines represent bare propagators of the charge bosons $\mathcal{A}_0^{ab}(r, \tau)$, the spin bosons $\mathcal{C}_0^{ab}(r, \tau)$, respectively, determined by $\hat{\mathcal{L}}_B^{(0)}$, in which self-energy effects are not taken into account. Thin lines with arrows stand for bare propagators of the quasiparticles $\mathcal{G}_{0\sigma}^{(f)}(r, \tau)$ determined by

$$\hat{\mathcal{L}}_0 = \sum_{ij} \hat{f}_{i\sigma}^\dagger(\tau) [\hat{D}_i \delta_{ij} + \zeta_{0\sigma} t_{ij}] \hat{f}_{j\sigma}(\tau), \quad (\text{A.18})$$

where $\zeta_{0\sigma} = g_{1\sigma}^2 g_{2\sigma}^2 (\bar{p}_{0\sigma} \bar{e}_0 + \bar{d}_0 \bar{p}_{0\sigma})^2$. The Lagrangian $\hat{\mathcal{L}}_0$ is obtained by decoupling the fluctuating bosons from the Lagrangian $\hat{\mathcal{L}}_0$ (Eq.(A.6)). Thick and thin dashed lines stand for the cofermions' propagators \mathcal{F}^{ab} and bare propagators $\mathcal{F}_0^{ab} = \delta_{a,b}/\epsilon$ ($\epsilon \rightarrow 0$), respectively.

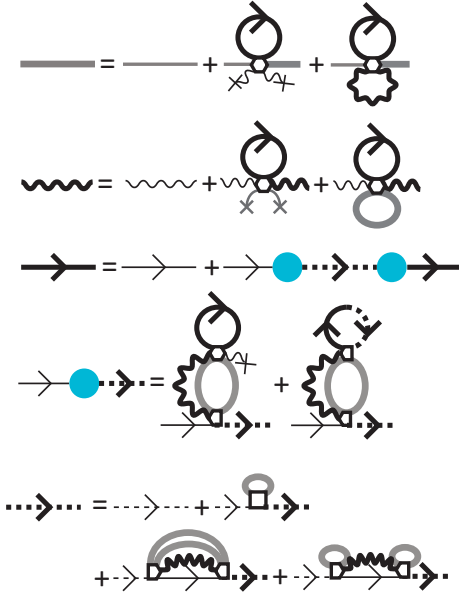


FIG. 7: (Same figure as Fig.1 in the main article) Diagrams for the Dyson equations. Solid and dashed lines with arrows represent propagators of the quasiparticles and cofermions, respectively. Thin wavy lines stand for the charge bosons, and thick solid lines are the spin bosons. Condensations of bosons are represented by lines terminated at crosses. Coupling constant $g_{1\sigma}^2 g_{2\sigma}^2 t_{ij}$ is represented by open polygons. Here, we do not distinguish holons and doublons. Spins are also not distinguished in the diagram, for simplicity.

In the set of Dyson equations (Fig.7), we neglect the coupling between charge and spin bosons described by propagators such as $\langle \tilde{p}_{i\sigma}^\dagger \tilde{e}_i \rangle$, at the Gaussian level, since these coupling terms are higher order contributions. Below we explain that the coupling gives higher order contribution with respect to hole-doping rate x , in proximity to Mott insulating states: Since operators including both charge and spin such as $\tilde{p}_{i\sigma}^\dagger \tilde{e}_i$ do not conserve the electric charge, propagators such as $\langle \tilde{p}_{i\sigma}^\dagger \tilde{e}_i \rangle$ should vanish in the

Mott insulating phase, where the charge can not fluctuate. Therefore, the charge and spin excitations are well separated in the Mott insulating phase.

When hole carriers are doped, $\tilde{p}_{i\sigma}^\dagger \tilde{e}_i$ can have a non zero expectation value, at most, scaled by condensate fraction of holons \bar{e}_0 which gives a rough estimate of the amplitude of charge fluctuations. From a relation $\bar{e}_0^2 \propto x$ held in the KR theory for the hole-doped case, we obtain $\langle \tilde{p}_{i\sigma}^\dagger \tilde{e}_i \rangle \propto \sqrt{x}$. Furthermore, there is an additional constraint for the coupling terms such as $\langle \tilde{p}_{i\sigma}^\dagger \tilde{e}_i \rangle$: they do not appear alone in calculations of physical quantities. To conserve charge and spin on average, $\langle \tilde{p}_{i\sigma}^\dagger \tilde{e}_i \rangle$ appears with $\langle \tilde{e}_i^\dagger \tilde{p}_{i\sigma} \rangle$ in pair, for example. Therefore, the contribution of the coupling between charge and spin bosons to physical quantities is scaled by $(\sqrt{x})^2$. It concludes that the coupling between the charge and spin bosons gives contributions as a higher order in terms of x in physical quantities.

By solving the set of the Dyson equations, we obtain the propagators for the quasiparticles and cofermions. Here the bosonic degrees of freedom are taken into account in self-consistent fashion, through the cofermion self-energy $\Sigma_\sigma^{(\text{cf})}(r, \tau)$, and the amplitude Δ_{ij} of hybridization between the quasiparticles and cofermions, each of which we detail below.

The Lagrangian for the cofermions is given by

$$\hat{\mathcal{L}}_{\text{cf}} = - \sum_{ij\sigma} \hat{\mathbf{Y}}_{i\sigma}^\dagger(\tau) \left[\Sigma_\sigma^{(\text{cf})}(r, \tau) \right] \hat{\mathbf{Y}}_{j\sigma}(\tau), \quad (\text{A.19})$$

where $\hat{\mathbf{Y}}_{i\sigma}^\dagger = (\hat{\psi}_{i\sigma}^\dagger, \hat{\chi}_{i\sigma}^\dagger)$ is a vector notation for the cofermions, as is defined in the main article, and $r = i - j$. The cofermion self-energy $\Sigma_\sigma^{(\text{cf})}(r, \tau)$ is a 2×2 symmetric matrix,

$$\Sigma_\sigma^{(\text{cf})} = \begin{bmatrix} \Sigma_\sigma^{11} & \Sigma_\sigma^{12} \\ \Sigma_\sigma^{21} & \Sigma_\sigma^{22} \end{bmatrix}. \quad (\text{A.20})$$

The hybridization between the quasiparticles and cofermions is described by

$$\hat{\mathcal{L}}_{\text{hyb}} = \sum_{i,j,\sigma} [\hat{\mathbf{Y}}_{i\sigma}^\dagger(\tau) \Delta_{ij} \hat{f}_{j\sigma}(\tau) + \hat{f}_{i\sigma}^\dagger(\tau) \Delta_{ij}^T \hat{\mathbf{Y}}_{j\sigma}(\tau)] \quad (\text{A.21})$$

where $\Delta_{ij}^T = (\Delta_{ij}^{(\psi)}, \Delta_{ij}^{(\chi)})$. As a result, the effective Lagrangian for the quasiparticles and cofermions, $\hat{\mathcal{L}}_{\text{eff}}$, is given as

$$\hat{\mathcal{L}}_{\text{eff}} = \hat{\mathcal{L}}_0 + \hat{\mathcal{L}}_{\text{cf}} + \hat{\mathcal{L}}_{\text{hyb}}. \quad (\text{A.22})$$

When the charge gap is relatively small, $\Sigma_\sigma^{11} \simeq \Sigma_\sigma^{22}$ and $\Delta_{ij}^{(\psi)} \simeq \Delta_{ij}^{(\chi)}$ hold approximately. When the charge gap collapses, $\Sigma_\sigma^{11} = \Sigma_\sigma^{22}$ and $\Delta_{ij}^{(\psi)} = \Delta_{ij}^{(\chi)}$ hold exactly. In our results, we employ the approximate relations $\Sigma = \Sigma_\sigma^{11} \simeq \Sigma_\sigma^{22}$ and $\Delta_{ij} = \Delta_{ij}^{(\psi)} \simeq \Delta_{ij}^{(\chi)}$. Then

a cofermion mode $(\hat{\psi}_{k\sigma} + \hat{\chi}_{k\sigma})/\sqrt{2}$ hybridize with quasiparticles through the amplitude $\Delta(k)$, which is depicted in Fig.7 as closed (blue) circles, where k is a momentum. The inverse of cofermion propagator (namely, the cofermion self-energy) for $(\hat{\psi}_{k\sigma} + \hat{\chi}_{k\sigma})/\sqrt{2}$ is given as

$$\frac{-1}{2}[\Sigma_{\sigma}(k, i\varepsilon_n) + \Sigma'_{\sigma}(k, i\varepsilon_n)] = \gamma_k i\varepsilon_n - \alpha_k + O(\varepsilon_n^2) \quad (\text{A.23})$$

where ε_n is a fermionic Matsubara frequency.

Then, the Green's function for the quasiparticles is given as

$$\begin{aligned} \mathcal{G}_{\sigma}^{(f)}(k, i\varepsilon_n \rightarrow \omega + i\delta) &= G_{\sigma}^{(f)}(k, \omega + i\delta) \\ &\simeq \left[\omega + i\delta - \zeta_{0\sigma} \epsilon_k + \mu - \frac{\Delta(k)^2}{\gamma_k(\omega + i\delta) - \alpha_k} \right]^{-1} \end{aligned} \quad (\text{A.24})$$

where ϵ_k is the Fourier transformation of t_{ij} , and μ is the chemical potential. Here we note that the weights of the two quasiparticle bands split by the zero surface defined by $\omega = \alpha_k/\gamma_k$ are not the same in our theory.

In our calculations, we define the doping rate x by using the quasiparticle Green's function as

$$1 - x = \lim_{T \rightarrow 0+} \frac{T}{N_s} \sum_{k, i\varepsilon_n, \sigma} \mathcal{G}_{\sigma}^{(f)}(k, i\varepsilon_n), \quad (\text{A.25})$$

where T stands for temperature and N_s is the number of sites.

The Green's function for the electrons, instead of the quasiparticles, is given as

$$\begin{aligned} \mathcal{G}_{ij\sigma}(\tau) &= -\langle T \hat{c}_{i\sigma}(\tau) \hat{c}_{j\sigma}^{\dagger}(0) \rangle \\ &\simeq -\langle T \hat{z}_{i\sigma}^{\dagger}(\tau) \hat{z}_{j\sigma}(0) \rangle \\ &\times \langle T \hat{f}_{i\sigma}(\tau) \hat{f}_{j\sigma}^{\dagger}(0) \rangle \\ &= \langle T \hat{z}_{i\sigma}^{\dagger}(\tau) \hat{z}_{j\sigma}(0) \rangle \mathcal{G}_{ij\sigma}^{(f)}(\tau), \end{aligned} \quad (\text{A.26})$$

where the bosonic and fermionic degrees of freedom are decoupled, because the resultant action in our theory does not contain the hybridization between bosons and fermions. The quasiparticle Green's function is defined, as in the previous sections, as

$$\mathcal{G}_{ij\sigma}^{(f)}(\tau) = -\langle T \hat{f}_{i\sigma}(\tau) \hat{f}_{j\sigma}^{\dagger}(0) \rangle. \quad (\text{A.27})$$

The bosonic part in Eq.(A.26) is given by

$$\begin{aligned} \langle T \hat{z}_{i\sigma}^{\dagger}(\tau) \hat{z}_{j\sigma}(0) \rangle &\simeq g_{1\sigma}^2 g_{2\sigma}^2 \langle T [\hat{\mathbf{b}}_i^{\dagger}(\tau) \cdot \hat{\mathbf{p}}_{i\sigma}(\tau)] \\ &\times [\hat{\mathbf{p}}_{j\sigma}^{\dagger}(\tau) \cdot \hat{\mathbf{b}}_j(\tau)] \rangle, \end{aligned} \quad (\text{A.28})$$

where we use vector notation as $\hat{\mathbf{b}}_i^{\dagger} = (\hat{e}_i^{\dagger}, \hat{d}_i^{\dagger})$, $\hat{\mathbf{p}}_{i\sigma}^{\dagger} = (\hat{p}_{i\sigma}^{\dagger}, \hat{p}_{i\bar{\sigma}}^{\dagger})$. Because we adopt the boson dynamics in

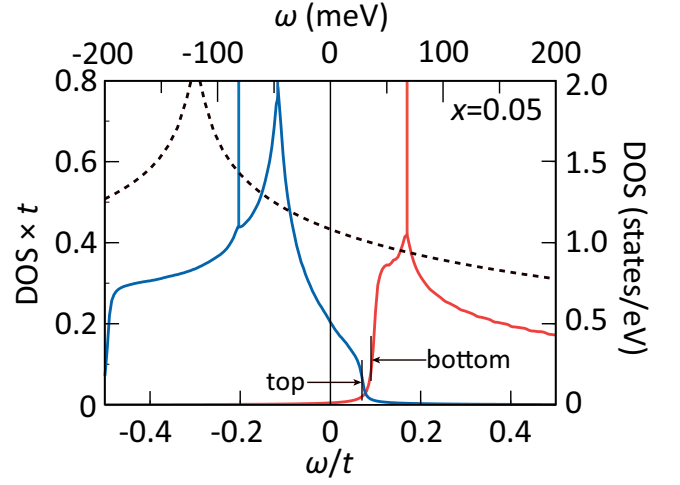


FIG. 8: Quasiparticle density of states (DOS). Solid curves show our result for DOS as function of ω for $x = 0.05$. Dashed curve shows DOS for the non-interacting case with the same band parameter $t' = 0.25t$ and the doping $x = 0.05$.

which charge and spin bosons are decoupled, this bosonic part of the Green's function is rewritten as

$$\begin{aligned} &\langle T \hat{z}_{i\sigma}^{\dagger}(\tau) \hat{z}_{j\sigma}(0) \rangle \\ &\simeq g_{1\sigma}^2 g_{2\sigma}^2 \langle T [\bar{\mathbf{b}}_0 \cdot \bar{\mathbf{p}}_{0\sigma}^T] [\bar{\mathbf{p}}_{0\sigma} \cdot \bar{\mathbf{b}}_0^T] \rangle \\ &+ g_{1\sigma}^2 g_{2\sigma}^2 \langle T [\tilde{\mathbf{b}}_i^{\dagger}(\tau) \cdot \tilde{\mathbf{p}}_{0\sigma}^T] [\bar{\mathbf{p}}_{0\sigma} \cdot \tilde{\mathbf{b}}_j(\tau)] \rangle \\ &+ g_{1\sigma}^2 g_{2\sigma}^2 \langle T [\bar{\mathbf{b}}_0 \cdot \tilde{\mathbf{p}}_{i\sigma}(\tau)] [\tilde{\mathbf{p}}_{j\sigma}^{\dagger}(\tau) \cdot \bar{\mathbf{b}}_0^T] \rangle \\ &+ g_{1\sigma}^2 g_{2\sigma}^2 \langle T [\tilde{\mathbf{b}}_i^{\dagger}(\tau) \cdot \tilde{\mathbf{p}}_{i\sigma}(\tau)] [\tilde{\mathbf{p}}_{j\sigma}^{\dagger}(\tau) \cdot \tilde{\mathbf{b}}_j(\tau)] \rangle \end{aligned} \quad (\text{A.29})$$

where $\bar{\mathbf{b}}_0 = (\bar{e}_0, \bar{d}_0)$ and $\bar{\mathbf{p}}_{0\sigma} = (\bar{p}_{0\sigma}, \bar{p}_{0\bar{\sigma}})$. If we retain only the first and second lines of the right hand side of Eq.(A.29), the electron Green's function is reduced to that already obtained in Ref.31. The contribution of the fourth line of the right hand side of Eq.(A.29) is small compared with these from other lines in Eq.(A.29), and we ignore the fourth term.

2. Supplementary result for quasiparticle density of states

Here we show supplementary results for the ω -dependence of the quasiparticle density of states (DOS). The ω -dependence of DOS (solid curves in Fig.8) shows significant asymmetry around $\omega = 0$ compared to the DOS for the non-interacting case (the dashed curve in Fig.8).

This asymmetry of the DOS naturally explain the asymmetric tunneling spectra with respect to the sign of the bias observed in the scanning tunneling microscopy (STM) measurements of the hole-underdoped

cuprates^{25,35}. Although in the STM measurements, the asymmetry is observed up to several hundreds meV, the present result offers a possible origin of the asymmetry observed especially up to 100 meV. Our result is in sharp contrast to the previous work by Anderson and Ong³², in which the quasiparticle weights of the states for the added electrons above μ and the states for the removed electrons below μ are different from each other. They claimed that the quasiparticle weights inevitably show a step-like singularity at the Fermi level in the proxim-

ity to Mott insulators. In our theory, such singularities at the Fermi level are not needed for occurrence of the asymmetric DOS. On the other hand, the recent study by Nieminen *et al.*, shows that layers other than the CuO₂ layers in cuprates³³ play a considerable role on the tunneling spectra and cause asymmetric spectra. Such effects of the layers other than the CuO₂ layers, which are ignored in our theory, will enhance the asymmetry of the tunneling spectra.

-
- * Electronic address: yamaji@solis.t.u-tokyo.ac.jp
- ¹ A. Damascelli, Z. Hussain, and Z.-X. Shen, *Rev. Mod. Phys.* **75**, 473 (2003).
 - ² T. Yoshida *et al.*, *Phys. Rev. B* **74**, 224510 (2006).
 - ³ J.-Q. Meng *et al.*, *Nature* **462**, 335 (2009).
 - ⁴ M. Imada, A. Fujimori, and Y. Tokura, *Rev. Mod. Phys.* **70**, 1039 (1998).
 - ⁵ J. Hubbard, *Proc. Roy. Soc.(London)* **A 281**, 401(1964).
 - ⁶ W.F. Brinkman and T.M. Rice, *Phys. Rev. B* **2**, 4302 (1970).
 - ⁷ W. Metzner and D. Vollhardt, *Phys. Rev. Lett.* **62**, 324 (1989).
 - ⁸ M. B. J. Meinders, H. Eskes, and G. A. Sawatzky, *Phys. Rev. B* **48**, 3916 (1993).
 - ⁹ P. A. Lee, N. Nagaosa, and X.-G. Wen, *Rev. Mod. Phys.* **78**, 17 (2006), and references therein.
 - ¹⁰ N. Furukawa, T. M. Rice, and M. Salmhofer, *Phys. Rev. Lett.* **81**, 3195 (1998).
 - ¹¹ I. Dzyaloshinskii, *Phys. Rev. B* **68**, 085113 (2003).
 - ¹² D. S  n  chal and A.-M. S. Tremblay, *Phys. Rev. Lett.* **92**, 126401 (2004).
 - ¹³ K.-Y. Yang, T. M. Rice, and F.-C. Zhang, *Phys. Rev. B* **73**, 174501 (2006).
 - ¹⁴ T. D. Stanescu and G. Kotliar, *Phys. Rev. B* **74**, 125110 (2006).
 - ¹⁵ S. Sakai, Y. Motome, and M. Imada, *Phys. Rev. Lett.* **102**, 056404 (2009); arXiv:1004.2569v1.
 - ¹⁶ P. Phillips, T.-P. Choy, and R. G. Leigh, *Rep. Prog. Phys.* **72**, 036501 (2009).
 - ¹⁷ G. D. Mahan, *Many-Particle Physics* (Kluwer Academic / Plenum Publishers, New York, 2000).
 - ¹⁸ B. I. Halperin and T. M. Rice, *Rev. Mod. Phys.* **40**, 755-766 (1968).
 - ¹⁹ S. Uchida *et al.*, *Phys. Rev. B* **43**, 7942-7954 (1991).
 - ²⁰ D. S. Ellis *et al.*, *Phys. Rev. B* **77**, 060501 (2008).
 - ²¹ R. Schuster *et al.*, *Phys. Rev. B* **79**, 214517 (2009).
 - ²² A. Ino *et al.*, *Phys. Rev. B* **65**, 094504 (2002).
 - ²³ J. W. Loram *et al.*, *J. Phys. Chem. Solids* **62**, 59 (2001).
 - ²⁴ N. Momono *et al.*, *Physica C* **233**, 395 (1994).
 - ²⁵ Ch. Renner *et al.*, *Phys. Rev. Lett.* **80**, 149 (1998).
 - ²⁶ R. W. Hill *et al.*, *Nature* **414**, 711 (2001).
 - ²⁷ C. Proust *et al.*, *Phys. Rev. B* **72**, 214511 (2005).
 - ²⁸ G. Kotliar and A. E. Ruckenstein, *Phys. Rev. Lett.* **57**, 1362 (1987).
 - ²⁹ F. Lechermann, A. Georges, G. Kotliar and O. Parcollet, *Phys. Rev. B* **76**, 155102 (2007).
 - ³⁰ C. Castellani *et al.*, *Phys. Rev. Lett.* **69**, 2009 (1992).
 - ³¹ R. Raimondi and C. Castellani, *Phys. Rev. B* **48**, 11453 (1993).
 - ³² P. W. Anderson and N. P. Ong, *J. Phys. Chem. Solids* **233**, 1 (2006).
 - ³³ J. Nieminen *et al.*, *Phys. Rev. Lett.* **102**, 037001 (2009).
 - ³⁴ T. Jolicoeur and J. C. Le Guillou, *Phys. Rev. B* **44**, 2403 (1991).
 - ³⁵ T. Hanaguri *et al.*, *Nature* **430**, 1001 (2004).